

Numerical Modelling of a Phase Change Material-based Shell and Tube Thermal Energy Storage Unit

Mansoureh Khaljani^{1,2}, Arslan Saleem¹, Hector Bastida¹, Jose Munoz Criollo¹, Carlos E. Ugalde-Loo¹, Robert Smart², Nick Jenkins¹

¹School of Engineering, Cardiff University, Cardiff, Wales, United Kingdom

²SRS Works Ltd, Berkshire, England, United Kingdom

KhaljaniM@cardiff.ac.uk, SaleemA7@cardiff.ac.uk, BastidaHernandezJH@cardiff.ac.uk, MunozCriolloJJ@cardiff.ac.uk, Ugalde-LooC@cardiff.ac.uk, Robert.Smart@srsworks.co.uk, JenkinsN6@cardiff.ac.uk

Abstract - Numerical modelling analysis is performed to assess the operation of a thermal energy storage unit. The system is comprised by a heat exchanger placed in a cubic case filled with phase change material (PCM). Water is used as the heat transfer fluid. In the charging process, hot water is circulated through the tubes of the heat exchanger and heat transferred to the PCM. The 3-D modelling is performed by solving unsteady Reynolds-averaged Navier-Stokes equations. The modelling approach allows a detailed analysis of the flow and thermal characteristics of the PCM and water in the thermal store.

Keywords: Thermal energy storage, phase change material, charging, numerical modelling.

1. Introduction

Climate change has increased the average ambient temperatures worldwide, causing severe heat waves and other extreme weather events. This has forced the world to develop innovative, energy-efficient, and reliable heating, cooling, and thermal energy storage (TES) solutions. The working principle of TES is simple: during low demand periods, the energy is stored, which can later be recovered when the demand is high, hence providing flexibility [1]. TES systems are typically categorised into sensible heat, latent heat, and thermochemical energy storage. The selection of the appropriate storage technology will depend on the energy demand and system design requirements. The latent heat storage alternative benefits from the high phase transition energy of phase change materials (PCMs). These TES systems have gained significant attention due to their isothermal operation properties, high energy density, and cost-effectiveness [2,3].

This paper presents a three-dimensional (3-D) model to investigate the charging process of a PCM-based TES system to explore, in detail, the flow and thermal characteristics of the PCM and the heat transfer fluid (HTF).

2. Thermodynamic cycle of the proposed thermal energy storage with PCM

Fig. 1(a) shows a simplified schematic of the TES system under study. During the charging process, water circulates through the tubes at an initial temperature of 348 K and a pressure of 2 bar. Heat is transferred from the water to the PCM surrounding the tubes. The phase of the PCM changes from solid to liquid and energy is stored.

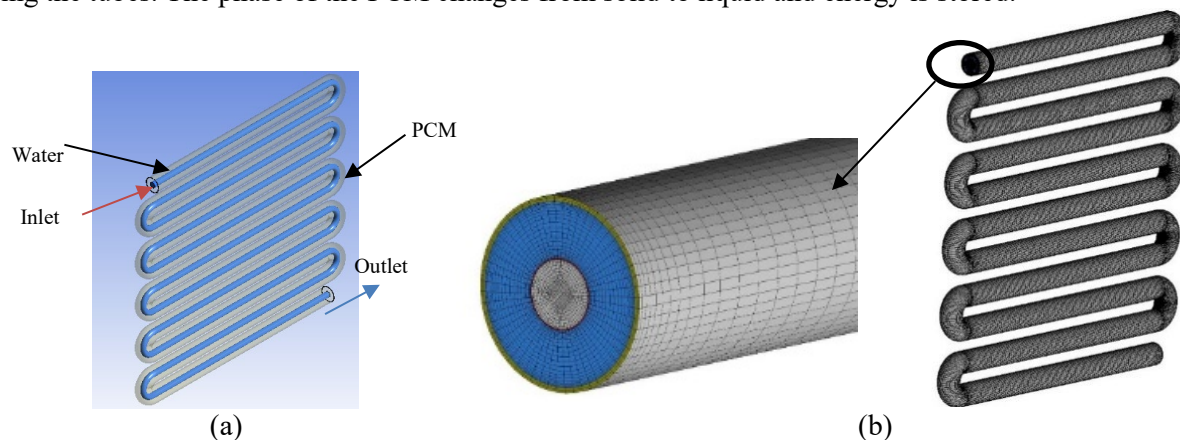


Fig. 1: (a) Simplified schematic of the TES unit. (b) Mesh generated for the 3-D simulation of the TES unit.

3. 3-D numerical modelling

3.1. Computational domain

The computational domain is a 3-D tube with a diameter of 6.75 mm. The tube consists of eleven copper U-shape tubes with a length of 270 mm and a diameter of 14 mm. The PCM surrounding the tubes has a diameter of 18 mm and is held inside a second tube with a thickness of 1 mm. The computational mesh was generated using Ansys® ICEM version 2019 R2c [4]. The mesh structure for the domain, which was generated for the tube and PCM, is presented in Fig. 1(b). The mesh density was adjusted by altering the global element size.

3.2 Governing equations and boundary conditions

The essential assumptions of the problem for numerical simulation are as follows:

- The fluid flow is laminar and incompressible.
- The properties of the HTF are kept constant.
- The outer wall of the geometry is assumed adiabatic.

By considering the above assumptions, the governing equations for the numerical analysis for continuity, Navier-Stokes, and energy in Cartesian coordinates are written as follows:

$$\nabla \cdot \vec{V} = 0 \quad (\text{continuity}) \quad (1)$$

$$\frac{\partial \rho \vec{V}}{\partial t} + \nabla \cdot (\rho \vec{V} \vec{V}) = -\nabla p + \mu \nabla^2 \vec{V} + S_B + S_m \quad (\text{momentum}) \quad (2)$$

$$\frac{\partial h_{sen}}{\partial t} + \frac{\partial h_{lat}}{\partial t} + \nabla \cdot (\vec{V} h_{sen}) = \nabla \cdot \left(\frac{k}{\rho c_p} \nabla h_{sen} \right) \quad (\text{energy}) \quad (3)$$

In (1), $\nabla \cdot$ is divergence and V indicates the velocity. In (2), the source term S_B , equal to $\rho g \beta (T - T_{ref})$, represents the change in density ρ causing natural convection and is implemented through the Boussinesq approximation. ∇p is the gradient of pressure, μ is the viscosity, and t is the time. S_m is a source term representing any added forces in a physical phenomenon and β is the expansion coefficient of a liquid relevant to a reference temperature T_{ref} . In (3), k is the thermal conductivity, c_p is the specific heat and h is the enthalpy. Subscript ‘sen’ is used to denote sensible, whereas ‘lat’ to denote latent.

The total enthalpy h_{tot} was obtained by adding the sensible heat h_{sen} and latent heat h_{lat} :

$$h_{tot} = h_{sen} + h_{lat} \quad (4)$$

$$\frac{\partial}{\partial t} (\rho H) + \nabla \cdot (\rho \vec{V} H) = \nabla \cdot (k \nabla T)$$

The following boundary conditions are used to solve the governing equations. Water enters the tube at a uniform speed (v_{in}) of 0.34 m/s and a temperature of 348 K. A no-slip condition is applied on the tube walls. The tube material is copper.

The thermophysical properties of the tubes, water, and PCM used in the simulations are given in Table 1. The initial PCM and water temperature was defined as 298.15 K.

Table 1: Thermophysical properties of PCM, water, and tube.

Material	Melting temperature (T) K	Density (ρ) kg/m ³	Specific Heat (c_p) J/kg·K	Viscosity (μ) kg/m·s
PCM	318-332	860	Variable	0.001013
Water	-	998	4182	0.001
Tube	-	8978	381	-

The commercial software Fluent® version 2020 R2 [4] was used to solve the set of governing equations and the associated boundary conditions. A 1st order implicit method was used on the transient formulation, and spatial derivatives were discretised using a second-order upwind scheme [5]. The simple algorithm [5] was adopted for pressure-velocity coupling. The 2nd order scheme was used to calculate the discretised pressure values on a staggered grid. The least

squares cell-based method was used to calculate the gradients of variables. The time step for all simulations was set up as 2×10^{-3} s.

4. Numerical results. Thermal behaviour analysis of the PCM in the TES unit

Fig. 2 illustrates the melting process of the PCM during charging, in terms of liquid fraction, as a function of charging time. The distribution of the liquid fraction is not uniform. The outer surface of the PCM closest to the tube walls melts first. After 3.5 min, the outer layer of the PCM has turned into liquid, while its inner parts have a solid-liquid co-existence. At 6.5 min, the PCM at the top of the tube is in the liquid phase, while the PCM at the bottom is still a liquid-solid mixture. This pattern may be due to natural convection, which transfers the PCM with a liquid phase towards the top of the tube during melting. At 11 min, most of the PCM has turned into liquid and the charging process has been completed.

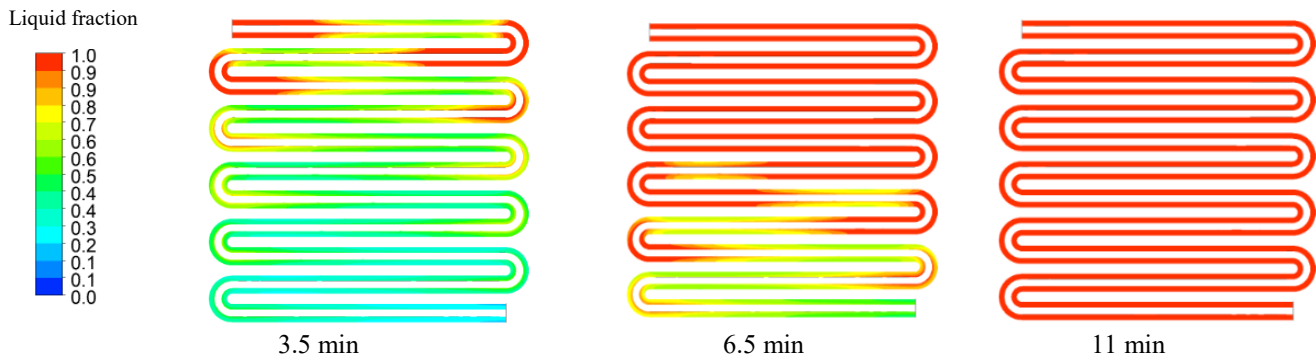


Fig. 2. Melting process of PCM during charging of TES.

Fig. 3 shows the temperature contour of the PCM. Like the liquid fraction, the distribution of temperature is not uniform during charging. At the inlet of the tube, the PCM melts first. Melting also occurs first at the curved sections of the tube due to the higher heat transfer rate between the HTF and PCM. At 3.5 min, the temperature of the PCM at the inner layer is higher than that at the outer layer of the tube. After 6.5 min, almost half of the PCM has melted as its temperature has reached the melting temperature. After 11 min, the temperature reaches 348 K and the charging process is completed.

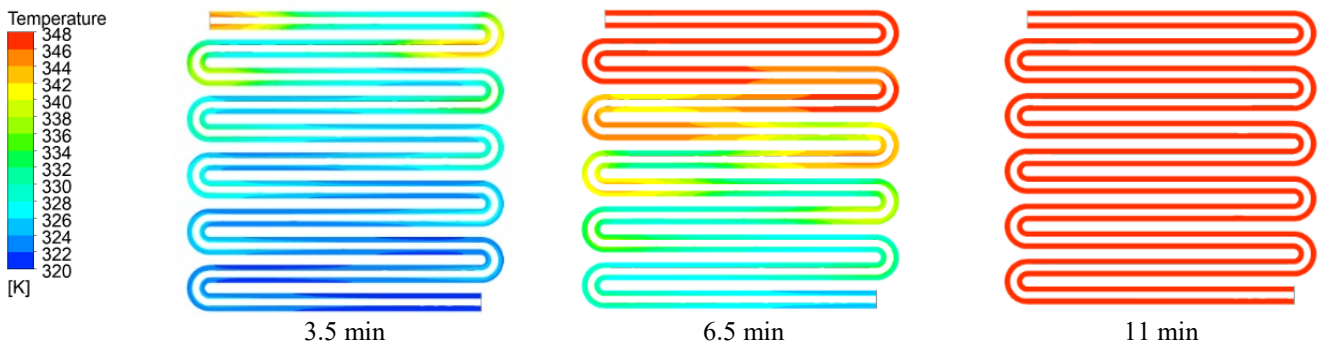


Fig. 3. Temperature contour of the PCM during charging

Fig. 4 shows the temperature profiles of the PCM during the charging process at the inlet, middle, and end of the tube. Charging starts from a homogeneous initial state of the entire system (PCM, tubes, and HTF). The system is initially at the set temperature of 298 K and the heat transfer inside the solid PCM is governed by conduction. After that, when the temperature range of the phase transition is reached, the melting process begins. During the phase transition, both conduction and natural convection in the liquid phase occurs. At the end of the phase transition, the PCM is in a liquid phase and the heat transfer inside the liquid PCM is governed by convection. As expected, the melting process of the PCM at the inlet of the tube is faster than that at the end of the tube.

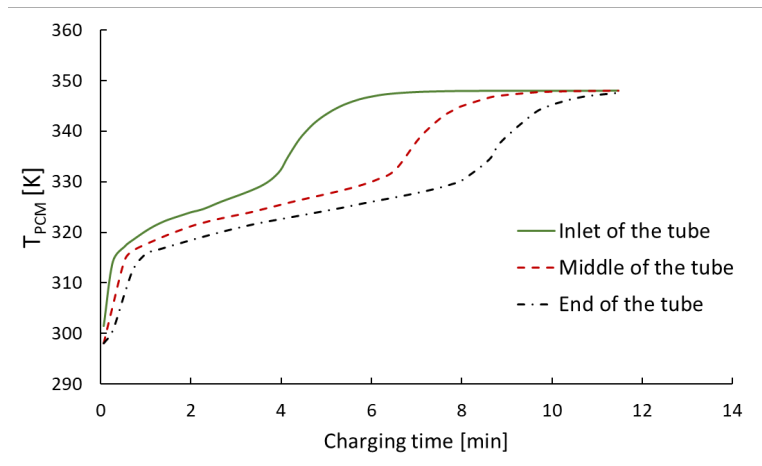


Fig. 4. Temperature profile of the PCM at different points of the tube.

Conclusions

This work investigated the flow and thermal characteristics of the PCM and HTF in a latent heat TES unit using a 3-D numerical modelling approach. The simulation results show that the distribution of the liquid fraction of the PCM is not uniform. The outer surface of the PCM closest to the tube walls melts first. The temperature contour for the PCM follows the same pattern as the liquid fraction. The PCM temperature is higher at the inlet of the tube and at the curved sections of the tube due to the higher heat transfer rate between the HTF and PCM.

The 3-D model provides very detailed results for the charging process of the TES system under study, but this analysis is computationally expensive. As future work, simulations of the discharging process will be conducted to fully characterise the TES unit. In addition, a 1-D model of the unit will be developed, and simulation results will be compared against those from the presented 3-D model. It is expected that the computation time required to solve the 1-D model will be considerably less. However, despite its reduced accuracy, the 1-D model may be useful for control system design, an easy estimation of the state-of-charge of the TES unit, and simulation of complex heating systems including TES systems.

Acknowledgments

This work was supported by InnovateUK, UK Research and Innovation, through the KTP project KTP012503 and by FLEXIS—a project part-funded by the European Regional Development Fund (ERDF), through the Welsh government (WEFO case number 80386).

References

- [1] A. Shukla, D. Buddhi, R.L. Sawhney, Solar water heaters with phase change material thermal energy storage medium: A review, *Renew. Sustain. Energy Rev.* 13 (2009) 2119–2125. <https://doi.org/10.1016/j.rser.2009.01.024>.
- [2] P.B. Salunkhe, P.S. Shembekar, A review on effect of phase change material encapsulation on the thermal performance of a system, *Renew. Sustain. Energy Rev.* 16 (2012) 5603–5616. <https://doi.org/10.1016/j.rser.2012.05.037>.
- [3] K.H. Solangi, S.N. Kazi, M.R. Luhur, A. Badarudin, A. Amiri, R. Sadri, M.N.M. Zubir, S. Gharehkhani, K.H. Teng, A comprehensive review of thermo-physical properties and convective heat transfer to nanofluids, *Energy* 89 (2015) 1065–1086. <https://doi.org/10.1016/j.energy.2015.06.105>.
- [4] F. Dadkhah, J. Zecher, *ANSYS Workbench Software Tutorial with Multimedia CD Release 12*, SDC Publications, 2009.
- [5] C. Zhang, P.Y. Li, J.D. Van De Ven, T.W. Simon, Design analysis of a liquid-piston compression chamber with application to compressed air energy storage, *Appl. Therm. Eng.* 101 (2016) 704–709. <https://doi.org/10.1016/j.applthermaleng.2016.01.082>.